Long-time dynamics and stationary nonequilibrium of an optically driven strongly confined quantum dot coupled to phonons

M. Glässl,[1,*] A. Vagov,[1] S. Lüker,[2] D. E. Reiter,[2] M. D. Croitoru,[1] P. Machnikowski,[3] V. M. Axt,[1] and T. Kuhn[2]

[1]*Institut für Theoretische Physik III, Universität Bayreuth, D-95440 Bayreuth, Germany*

[2]*Institut für Festkörpertheorie, Universität Münster, D-48149 Münster, Germany*

[3]*Institute of Physics, Wrocław University of Technology, PL-50-370 Wrocław, Poland*

(Received 5 July 2011; published 8 November 2011)

We study the long-time dynamics and the stationary nonequilibrium state of an optically driven quantum dot coupled to acoustic phonons using numerically exact real-time path integrals and a fourth-order correlation expansion. By exploring wide ranges of temperatures, carrier-phonon and carrier-light coupling strengths, we characterize the stationary nonequilibrium state and compare the exact solution to known, approximatively derived results. It is found that analytical calculations tend to overestimate the influence of the carrier-phonon coupling, particularly at low temperatures and in the weak-coupling regime. The possibility of controlling the dot occupation in the stationary nonequilibrium by varying the laser detuning is discussed. A comparison between the numerical methods identifies the range of validity of the correlation expansion, which in the long-time limit is found to be surprisingly wide.

DOI: 10.1103/PhysRevB.84.195311 PACS number(s): 03.65.Yz, 78.67.Hc, 63.22.−m

I. INTRODUCTION

The dissipative dynamics in coherently driven quantum dots (QDs) currently attracts much interest in experimental investigations as well as in theoretical studies. In particular, much effort has been devoted to better understand and characterize the damping of laser-driven excitonic Rabi oscillations (ROs),[1–10] which presents a prime obstacle to achieving coherent manipulations of the quantum states in the QD.[11,12] Recent experiments[4,5] identified the pure dephasing coupling of carrier states to bulklike acoustic phonons[13] as the principle source of dephasing and confirmed theoretically predicted results, such as a phonon-induced renormalization of the Rabi frequency[1,2] or a nonmonotonic dependence of the damping on the driving strength.[3,9]

The decoherence of a continuously laser-driven QD reflected in the decay of ROs strongly depends on temperature and excitation conditions. Typically it takes place on time scales from 10 to 100 ps. On the one hand, these times are much longer than the characteristic time of the initial phonon-induced dephasing after ultrafast excitation by a single pulse. This time can be roughly estimated as the time a phonon needs to pass the QD and is of the order of 1 ps. On the other hand, the time scale of the decay of ROs is still much shorter than typical time scales of other mechanisms, such as the recombination of excitons.[14,15] With the lifetime of excitons in QDs ranging from a few hundred picoseconds to roughly one nanosecond,[14] the dynamics of a continuously driven QD evolves on two characteristic time scales: first, the system is driven to a stationary nonequilibrium state performing damped ROs, and afterwards it relaxes at a much slower rate to a possibly different stationary nonequilibrium state.

The main aim of our work is to characterize the stationary nonequilibrium state that is reached due to the phonon-induced decoherence under optical driving with constant amplitude (cw excitation) at intermediate times. This differs from related works[1–7,9] that focused on the phonon-influenced dynamics under pulsed excitation on shorter time scales.

Theoretical studies of the dynamics of a strongly confined QD influenced by the carrier-phonon interaction are conventionally done using models in which few optically active electronic states are diagonally coupled to a continuum of bulk phonon modes. As this pure dephasing mechanism is dominant,[4,16] many details of the relaxation to the stationary nonequilibrium can be extracted from modeling the time evolution considering only this mechanism. When the carrier states are separated by large energy gaps and the frequency of the excitation is tuned close to resonance with one of the transition energies, the system can be reasonably well described by accounting for only two optically active levels. In the literature, an externally driven two-level system diagonally coupled to phonons has been discussed extensively in relation to various systems in physics and chemistry,[17,18] often related to dissipative quantum tunneling.

It has long been conjectured that if such a phonon-coupled two-level system is continuously driven, the reduced electronic density matrix will thermalize in a certain basis.[19] Once this nonequilibrium state is introduced, the relaxation dynamics can be easily described by the Bloch equations for the dissipative two-level system.[18,20,21] It should be noted, however, that within a Markovian approach, the basis is chosen by hand and this choice may be ambiguous, particularly when the carrier-phonon coupling is not weak. Numerical calculations not invoking the Markov approximation revealed that in the case of ohmic phonon coupling and small coupling constants (Kondo parameter), the density matrix is close to becoming diagonal in the basis formed by the dot-photon dressed states.[22–24] An approximate analytical result[17] for the stationary nonequilibrium state was later obtained by going beyond the noninteracting-blip approximation,[18,25] including a prediction of how the strength of the carrier-phonon coupling influences the long-time behavior. In the limit of a vanishing coupling strength, the obtained expression reduces to a thermal occupation of the dot-photon dressed states. The validity of this extended weak-coupling theory is restricted to low temperatures and weak phonon couplings.

To study the long-time dynamics in optically driven quantum dots for arbitrary carrier-phonon coupling strengths, we adapted a numerically exact quasi-adiabatic path-integral method[22,23,26,27] for the superohmic case.[28] This gives us the unique opportunity to characterize the stationary nonequilibrium of a many-particle system without any prejudice. We compare our results with known theoretical predictions based on approximations of different complexity and demonstrate that for a surprisingly wide range of parameters, the nonequilibrium state is close to a thermal occupation of the dot-photon dressed states. In addition, we show that the experimentally measurable dot occupation in the stationary nonequilibrium state can be controlled by a frequency detuning of the optical driving. Finally, we compare exact real-time path-integral results with those of a fourth-order correlation expansion approach.[2,29,30] Although this level of the correlation expansion is one of the most accurate approximative methods usually available to treat the dynamics of correlated systems, the question of whether residual errors accumulate and thus limit the prediction for the long-time behavior is still open. Thus, a comparison in the domain of long times, including the regimes of high temperatures and strong couplings, provides valuable information on its validity.

The paper is organized as follows. In Sec. II we introduce the model. The long-time evolution of the electronic system and its stationary nonequilibrium state is presented in Sec. III. Within the comparison of the numerical approaches, several technical issues for both calculation methods are discussed. Finally, some concluding remarks are presented in Sec. IV.

II. MODEL

We consider a strongly confined GaAs QD diagonally coupled to a continuum of delocalized acoustic phonons and driven by an external laser field. The corresponding Hamiltonian can be written as

$$H = H_{\text{dot}} + H_{\text{phonon}} + H_{\text{dot-phonon}} + H_{\text{dot-light}}, \tag{1}$$

where H_{dot} describes the electronic structure of the dot, H_{phonon} is the free phonon Hamiltonian, $H_{\text{dot-phonon}}$ represents the carrier-phonon coupling, and $H_{\text{dot-light}}$ represents the carrier-light coupling. As for strongly confined semiconductor QDs the electronic single-particle states are energetically well separated, we can safely neglect a Coulomb-induced mixing of states with different single-particle energies and, choosing circularly polarized light, we can restrict our analysis to two electronic levels. We take the unexcited ground state $|0\rangle$ as the zero of energy and define the energy gap between $|0\rangle$ and the single-exciton state $|1\rangle$ by $\hbar\omega_X$. Thus, H_{dot} reads

$$H_{\text{dot}} = \tfrac{1}{2}\hbar\,\omega_X\,(\mathbb{1} - \sigma_z), \tag{2}$$

where σ_z is a Pauli matrix. With $b_{\mathbf{q}}^\dagger$ ($b_{\mathbf{q}}$) representing the creation (annihilation) operator of a phonon with a wave vector $\mathbf{q}$ and energy $\hbar\omega_{\mathbf{q}}$, the free phonon Hamiltonian is given by

$$H_{\text{phonon}} = \hbar \sum_{\mathbf{q}} \omega_{\mathbf{q}} b_{\mathbf{q}}^\dagger b_{\mathbf{q}}, \tag{3}$$

and the pure dephasing carrier-phonon interaction reads

$$H_{\text{dot-phonon}} = \frac{1}{2}(\mathbb{1} - \sigma_z) \sum_{\mathbf{q}} (\gamma_{\mathbf{q}}^* b_{\mathbf{q}} + \gamma_{\mathbf{q}} b_{\mathbf{q}}^\dagger). \tag{4}$$

Here, $\gamma_{\mathbf{q}}$ denote the dot-phonon coupling constants that depend on the specific coupling type and the carrier wave functions as presented in detail in Ref. 29. As for GaAs self-assembled QDs the deformation potential coupling to longitudinal acoustic phonons provides by far the largest contribution to pure dephasing we concentrate on this mechanism and assume the dispersion relation to be linear, $\omega_{\mathbf{q}} = v_c|\mathbf{q}|$, where v_c is the sound velocity. For simplicity, we consider spherical dots with wave functions given by the ground-state solution of a harmonic potential, i.e.,

$$\psi_{e(h)}(\mathbf{r}) = \frac{1}{\pi^{3/4} a_{e(h)}^{3/2}} \exp\left(-\frac{r^2}{2a_{e(h)}^2}\right), \tag{5}$$

where $a_{e(h)}$ are the localization lengths of electrons and holes, respectively. The spectral density of the phonon bath is then given by[29]

$$J(\omega) = \frac{\omega^3}{4\pi^2\rho\hbar v_c^5}\left\{D_e \exp\left(-\frac{\omega^2 a_e^2}{4v_c^2}\right) - D_h \exp\left(-\frac{\omega^2 a_h^2}{4v_c^2}\right)\right\}^2, \tag{6}$$

where $D_{e(h)}$ denote the deformation potential constants and ρ is the density of the material. In the low-frequency limit, $J(\omega)$ scales as ω^3 and is thus of the superohmic type. For our calculations, we choose $a_e = 3$ nm and set $a_h = 0.87a_e$. All other material parameters are taken from Ref. 29. Let us finally turn to $H_{\text{dot-light}}$. Within the usual dipole and rotating wave approximation (RWA), the interaction with the classical light field $\mathbf{E}$ takes the form

$$H_{\text{dot-light}} = \mathbf{d} \cdot \mathbf{E}^{(+)}(t)\,\sigma_+ + \mathbf{d}^* \cdot \mathbf{E}^{(-)}(t)\,\sigma_-, \tag{7}$$

where $\sigma_\pm = \sigma_x \pm i\sigma_y$, $\mathbf{d}$ is the transition dipole moment, and $\mathbf{E}^{(\pm)}$ denote the positive and negative frequency components of the electric field. We set

$$\mathbf{d} \cdot \mathbf{E}^{(+)}(t) = \frac{\hbar}{2} f(t) e^{-i(\omega+\Delta/\hbar)t}. \tag{8}$$

The real envelope function $f(t)$ represents the instantaneous Rabi frequency, ω denotes the frequency resonant to the polaron-shifted exciton transition,[29] and Δ is a detuning. In the following, we will consider the case of constant optical driving, i.e., we assume cw excitation with $f(t) = \text{const}$ and, for brevity, refer to f as the field strength.

III. RESULTS

To study the long-time behavior of a continuously driven QD, we first present results obtained by using a numerical real-time path-integral approach.[22,28] In contrast to other widely used methods, the path-integral formalism is numerically exact and yields trustable results at arbitrarily long times, where the validity of approximate methods is *a priori* unclear. For the system under consideration, real-time path integrals are particularly suitable as the environment coupling is superohmic. This leads to a finite memory length and allows for a numerical memory truncation scheme. While

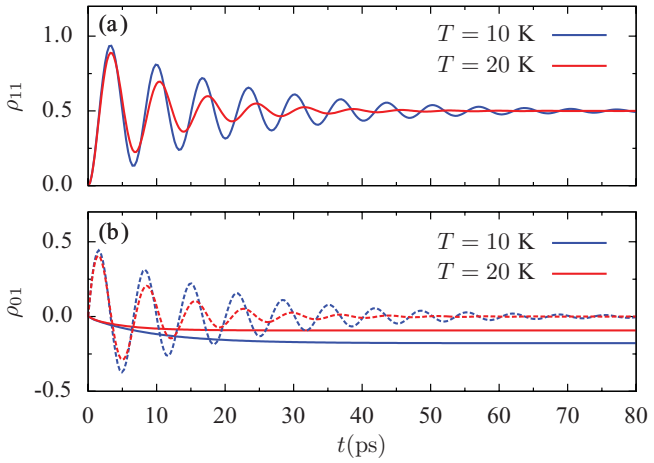

FIG. 1. (Color online) Temporal evolution of the density-matrix elements (a) ρ_{11} (occupation of the upper level) and (b) ρ_{01} (coherence) for $\Delta = 0$ and $f = 1.0$ ps^{-1} at $T = 10$ (blue lines) and 20 K (red lines). In (b), solid lines represent the real part of ρ_{01}, while dashed lines represent the imaginary part.

for ohmic or subohmic couplings such truncation schemes introduce qualitative changes in the long-time behavior, in the superohmic case the complete time evolution can be correctly reproduced.[28] The accuracy of the calculations solely depends on the chosen time step and the memory truncation length, and is therefore well controllable. A detailed description of our algorithm is given in Ref. 28.

We assume that the system is initially in a product state, with the electronic subsystem being in the ground state without an electron-hole pair and the phonons being in the thermal state at temperature T. At $t = 0$ ps, a laser with constant field strength f is switched on. Figure 1 shows the subsequent temporal evolution of the electronic system in the rotating frame for resonant driving, i.e., for $\Delta = 0$, with $f = 1.0$ ps^{-1} at $T = 10$ (blue lines) and 20 K (red lines). Plotted in Fig. 1(a) is the occupation of the upper level ρ_{11}, while the complex valued coherence ρ_{01}, which is related to the polarization vector $\mathbf{P}$ via $\mathbf{P} = \mathrm{Re}\,(\mathbf{d}\,\rho_{01})$, is shown in Fig. 1(b). Together, both quantities fully characterize the electronic degrees of freedom. The QD occupation performs phonon-damped ROs until it approaches the stationary and temperature-independent value $\rho_{11}(\infty) = 1/2$. For higher temperatures, the damping is enhanced and the stationary state is reached faster. The imaginary part of the coherence (dashed lines) shows similarly damped oscillations and vanishes in the limit of long times. In contrast, the real part of ρ_{01} (solid lines) decreases monotonically and reaches a temperature-dependent finite value. The latter clearly demonstrates that the electronic system does not become diagonal in the basis given by the eigenstates of H_{dot}.

Naturally, the question arises what defines the long-time behavior and whether there is a basis in which the system thermalizes. Quite generally, when a system can be decomposed into a set of stable quasiparticles and bath degrees of freedom that have a sufficiently weak coupling to the quasiparticles, the common expectation is that in the long-time limit, the bath coupling leads to a thermal occupation of the quasiparticle states. In our case, such a decomposition is suggestive when the carrier-phonon coupling is weak. Then the phonons provide the bath, and in the stationary state, a thermal occupation of the eigenstates of $H_0 = H_{\mathrm{dot}} + H_{\mathrm{dot-light}}$ that are referred to as dot-photon dressed states is expected.[18,20,21] In the rotating frame, H_0 is time independent and reads

$$H_0 = \tfrac{1}{2}\Delta(\sigma_z - \mathbb{1}) + \tfrac{1}{2}\hbar f \sigma_x. \tag{9}$$

With the abbreviation

$$\Omega = \sqrt{\Delta^2/\hbar^2 + f^2}, \tag{10}$$

the reduced density matrix for a thermal occupation of the dot-photon dressed states written in the eigenbasis of H_{dot} is given by

$$\rho^{(\mathrm{ds})} = \frac{1}{2}\mathbb{1} - \frac{1}{2\Omega}\tanh\left(\frac{\hbar\Omega}{2k_B T}\right)\left(\frac{\Delta}{\hbar}\sigma_z + f\sigma_x\right). \tag{11}$$

To check how close a thermal occupation of the dot-photon dressed states is to the exact stationary state, we compare in Fig. 2 numerically obtained results (crosses) with the prediction made by Eq. (11) (lines). Shown is the stationary value of the off-diagonal element $\rho_{01}(\infty)$ as a function of temperature for resonant driving, i.e., for $\Delta = 0$, at two field strengths, namely, at $f = 0.5$ (red line) and 1.0 ps^{-1} (blue line). Over the full temperature range, a quite convincing agreement can be found, indicating that the system is close to thermalization in the basis formed by the dot-photon dressed states. Consideration of the phonons as a bath requires that the carrier-phonon coupling can be treated as a small perturbation and, thus, *a priori*, this agreement had to be expected only for low temperatures, as for higher temperatures multiphonon processes gain importance even for weak carrier-phonon couplings.[29] Although the prediction that the system relaxes to a thermal occupation of the dot-photon dressed states is essentially confirmed, there are slight deviations, which are, surprisingly, most clearly visible in the range of small temperatures (see inset). We will come back to these deviations below. For the diagonal elements, the prediction

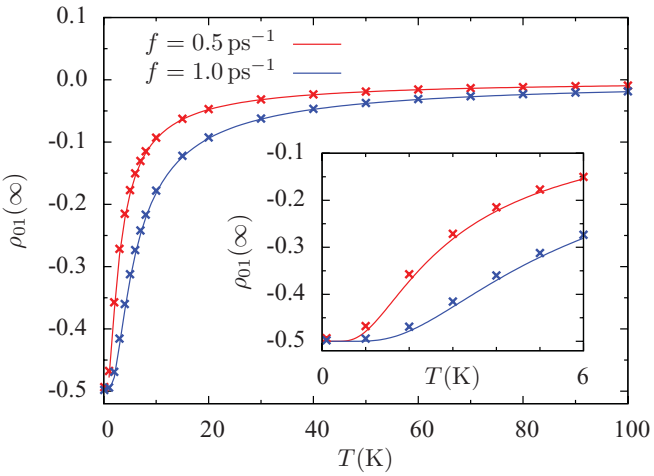

FIG. 2. (Color online) Stationary value of ρ_{01} as a function of temperature for resonant driving ($\Delta = 0$) with field strengths of $f = 0.5$ (red line) and 1.0 ps^{-1} (blue line). Solid lines correspond to a thermal occupation in the basis of the dot-photon dressed states; crosses represent path-integral results. The inset shows a zoom into the region of low temperatures.

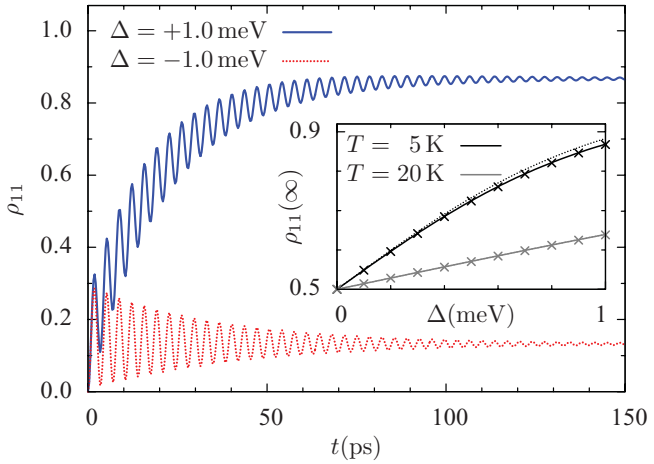

FIG. 3. (Color online) QD occupation ρ_{11} as a function of time at $T = 5$ K and $f = 1.0$ ps^{-1} for two different detunings of $\Delta = 1.0$ (blue solid line) and -1.0 meV (red dotted line). The inset shows the stationary value of ρ_{11} as a function of the detuning at $T = 5$ (black line) and 20 K (gray line). Solid and dotted lines correspond to a thermal occupation of the dressed states [Eq. (11)] and to the weak-coupling theory [Eq. (13a)], respectively. Crosses represent path-integral results.

$\rho_{00}(\infty) = \rho_{11}(\infty) = \frac{1}{2}$ of Eq. (11) for the case $\Delta = 0$ is in excellent agreement with the path-integral results for all temperatures and laser intensities (not shown).

Let us now turn to the case of off-resonant driving. Shown in Fig. 3 is the QD occupation ρ_{11} as a function of time at $T = 5$ K and $f = 1.0$ ps^{-1} for two representative values of the detuning, $\Delta = 1.0$ (blue solid line) and -1.0 meV (red dotted line), respectively. In contrast to resonant excitation [cf. Fig. 1(a)], the envelope functions of ROs are not symmetric and, most interestingly, for positive values of the detuning (i.e., the laser frequency exceeds the QD transition frequency) in the long-time limit, the QD occupation is higher than in the case of resonant driving. Here, for $T = 5$ K and $\Delta = 1.0$ meV, i.e., a detuning that is much smaller than ω_X such that the RWA is still valid, a final occupation of $\rho_{11} \simeq 0.84$ is found. Increasing the detuning or lowering the temperature leads to even higher occupations, which can be arbitrarily close to one. We would like to mention that a similar population inversion has been observed experimentally for a two-dot system in Refs. 31 and 32. Unlike the related theoretical study in Ref. 33, we find that in our model, the population inversion appears for superquadratic coupling [$J(\omega)$ scales as ω^3 for $\omega \to 0$]. Here, the magnitude of the effect only weakly depends on the strength of the carrier-phonon coupling, and the results presented in Fig. 3 can with good accuracy be derived from the assumption of a thermal occupation in the basis of the dot-photon dressed states. To show this, we compare in the inset of Fig. 3 the detuning-dependent stationary value of ρ_{11} at $T = 5$ (black line) and 20 K (gray line), as predicted by Eq. (11) (solid lines) and obtained numerically (crosses). An excellent agreement without any noticeable differences can be found. The additionally displayed dotted lines represent results of an extended weak-coupling theory and will be discussed below. Comparing the off-diagonal elements for finite values of Δ (not shown), the agreement is not just as well as for the diagonal elements, and we find similar deviations from the prediction of Eq. (11) as shown in Fig. 2 for the case of resonant driving. In the following, we will concentrate on these deviations.

When $\gamma_{\mathbf{q}}$ is not negligibly small, the role of phonons is not restricted to providing a redistribution of the quasiparticle occupations. Instead, they now also contribute to the definition of the stable quasiparticles, which become a superposition of carrier and phonon degrees of freedom, i.e., the quasiparticles assume a polaronic character. Recently, it has been shown within advanced master-equation approaches that accounting for polaronic effects substantially improves the description of the driven dynamics, in particular when the coupling is not weak.[6,7,34] It is clear that when the quasiparticles assume a polaronic character, the stationary reduced density matrix can no longer be independent on $\gamma_{\mathbf{q}}$. Previous studies have worked out $\gamma_{\mathbf{q}}$-dependent corrections to Eq. (11). In particular, in Ref. 17, an extended weak-coupling theory has been derived for the temperature regime

$$T \lesssim \hbar\Omega/k_B, \tag{12}$$

which goes beyond the noninteracting blip approximation (NIBA) by dealing systematically with interblip correlations to the first order in the coupling strength. The corresponding prediction for the stationary electronic density matrix is

$$\rho(\infty) = \frac{1}{2}\mathbb{1} - \frac{1}{2\Omega_b}\tanh\left(\frac{\hbar\Omega_b}{2k_BT}\right)\left(\frac{\Delta}{\hbar}\sigma_z + \frac{f_{\text{eff}}^2}{f}\sigma_x\right), \tag{13a}$$

where

$$\Omega_b = \left(\Delta^2/\hbar^2 + f_{\text{eff}}^2\right)^{1/2}, \tag{13b}$$

and f_{eff} depends on the coupling strength via

$$f_{\text{eff}} = f\exp\left(-\frac{1}{2}\sum_{\mathbf{q}}\frac{\gamma_{\mathbf{q}}^2}{\omega_{\mathbf{q}}^2}\right). \tag{13c}$$

A detailed derivation is presented in Ref. 17.

Obviously, in the limit $\gamma_{\mathbf{q}} \to 0$, Eq. (13a) simplifies to Eq. (11). It is instructive to compare our numerically exact calculations with the perturbatively derived result of the weak-coupling theory, which should be applicable for GaAs parameters. Such a comparison will show whether or not the deviations from a thermal occupation of the dot-photon dressed states, as seen in Fig. 2, can be traced back to the finite strength of the carrier-phonon coupling. Plotted in Fig. 4 is the stationary value of the off-diagonal element $\rho_{01}(\infty)$ as a function of temperature at two field strengths of $f = 0.5$ (red lines) and 1.0 ps^{-1} (blue lines) for the case of resonant excitation. Solid lines represent path-integral results, squares display results of a fourth-order correlation expansion that will be discussed later in the paper, dashed lines correspond to a thermal occupation of the dot-photon dressed states [Eq. (11)], and dotted lines correspond to the weak-coupling theory given in Eq. (13a). According to Eq. (12), the latter should be valid up to $T = 3.5$ and 7 K for $f = 0.5$ and 1.0 ps^{-1}, respectively. It is clearly seen that at all temperatures and for both laser intensities, the path-integral results are in between the predictions of Eqs. (11) and (13a). While a thermal occupation of the dot-photon dressed states assumes slightly lower values, the weak-coupling theory overestimates

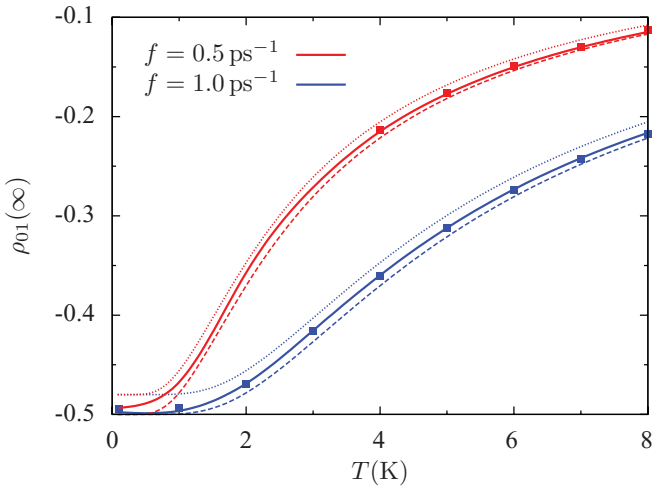

FIG. 4. (Color online) Stationary value of ρ_{01} as a function of temperature for resonant driving ($\Delta = 0$) with $f = 0.5$ (red lines) and 1.0 ps^{-1} (blue lines). Dashed and dotted lines correspond to a thermal occupation of the dot-photon dressed states [Eq. (11)] and to the weak-coupling theory [Eq. (13a)], respectively. Solid lines show path-integral results; squares represent results of a fourth-order correlation expansion.

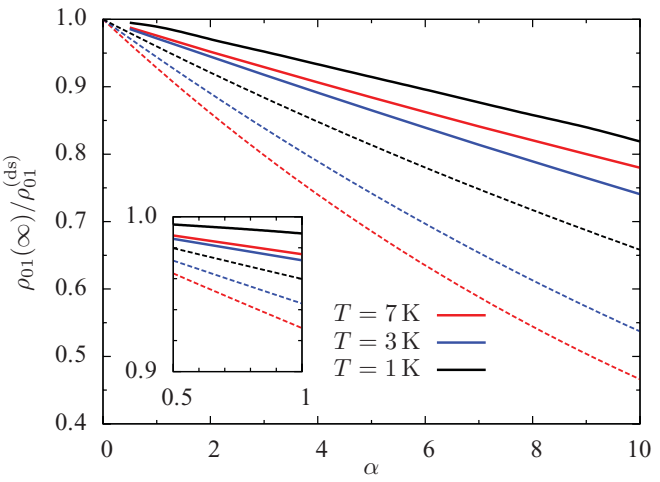

FIG. 5. (Color online) Deviations from the stationary value of ρ_{01} from the dressed-state expectation $\rho_{01}^{(\mathrm{ds})}$ as a function of the coupling strength (in units of the unscaled carrier-phonon coupling of GaAs) for resonant driving ($\Delta = 0$) with $f = 1.0$ ps^{-1} at different temperatures (see key). Solid lines represent path-integral results; dashed lines display the prediction made by Eq. (13a). The inset shows a zoom into the weak-coupling regime.

the dependency on the coupling strength and assumes slightly higher ones. We would like to stress that the driving strengths of $f = 0.5$ and 1.0 ps^{-1} chosen in our simulations are well below the frequency $f \sim 2.5$ ps^{-1} at which the environmental spectral density [cf. Eq. (6)] is maximal. Thus, the diminished polaronic character of the stationary state with respect to Eq. (13a) is not due to a too strong driving that would exceed the cutoff frequency of the phonon bath.

For temperatures exceeding those given by Eq. (12), the path-integral results are much closer to a thermal occupation of the dot-photon dressed states than to Eq. (13a). Interestingly, this is also true in the limit of very low temperatures, and thus we find that the temperature range where Eq. (13a) yields a better description than Eq. (11) is rather small. However, even if the weak-coupling theory is not in quantitative agreement with the exact calculations, the coupling-strength-induced corrections with respect to Eq. (11) show the correct tendency and suggest that the equilibrium will be the closer to a thermal state in the dot-photon dressed basis the smaller the carrier-phonon coupling is.

To prove the validity of this conclusion and to analyze up to which coupling strengths one can trust Eq. (13a), we performed calculations for different values of the carrier-phonon coupling. To this end, we scaled $|\gamma_{\mathbf{q}}|^2$ by hand by a factor α varying from $\alpha = 0.5$ up to 10. While unscaled GaAs parameters, i.e., $\alpha = 1$, represent the low-coupling limit, a tenfold stronger coupling roughly simulates the strength of acoustic phonon coupling in GaN,[35] which provides a benchmark material for enhanced coupling. Plotted in Fig. 5 is the stationary value of ρ_{01} normalized by the dressed-state expectation $\rho_{01}^{(\mathrm{ds})}$ as a function of α for resonant driving with $f = 1.0$ ps^{-1} at temperatures of $T = 7$ (red line), 3 (blue line), and 1 K (black line). For each temperature, solid lines represent path-integral data, while dashed lines have been calculated according to Eq. (13a). Note that a thermal occupation in the basis of the dot-photon dressed states would correspond to $\rho_{01}(\infty)/\rho_{01}^{(\mathrm{ds})} = 1$. It is clearly seen that the deviations of $\rho_{01}^{(\mathrm{ds})}$ from the exact results increase with rising strength of the carrier-phonon coupling and vanish for $\alpha \to 0^+$. Of course, in the limit $\alpha = 0$, no stationary state will be reached, as in this case our model system would experience no damping but everlasting ROs. Nevertheless, the path-integral results suggest that for a finite but arbitrarily small carrier-phonon coupling, the equilibrium state will indeed be given by a thermal occupation of the dot-photon dressed states. It is remarkable that although this limit is in accordance with the weak-coupling theory, Eq. (13a) overestimates the dependence on the coupling strength not only for $\alpha \gg 1$, but also in the weak-coupling limit, as shown in the inset of Fig. 5. In the latter regime, the exact results for 1 and 7 K are closer to one, i.e., to Eq. (11), than to Eq. (13a). For 3 K, the path-integral data are almost equally far from both predictions. Thus, we find that the deviations of $\rho_{01}(\infty)/\rho_{01}^{(\mathrm{ds})}$ from one depend nonmonotonically on the temperature. The latter holds also in the strong-coupling regime. As can be seen, the weak-coupling theory predicts a convex dependence on α, while we find a dependence which is close to being linear. Because of this difference, in the strong-coupling regime, the equilibrium is better estimated by Eq. (13a).

In the previous discussion, we focused on off-diagonal elements and demonstrated that for nearly all temperatures in the weak-coupling regime, Eq. (11) provides a more accurate description than Eq. (13a). A similar conclusion can be drawn for diagonal elements. In the inset of Fig. 3, we discussed the detuning dependence of ρ_{11} and found an excellent agreement between path-integral data (crosses) and Eq. (11) (solid lines). For $T = 5$ K (black lines), where Eq. (13a) should be valid, we added the prediction of the weak-coupling theory as a dotted line. With rising values of the detuning, small discrepancies emerge, demonstrating that the bare dressed-state assumption

yields again a better estimate. For $T = 20$ K, the differences between Eqs. (11) and (13a) are tiny and both lines coincide.

So far, we have presented results obtained by using numerically exact real-time path integrals. Usually, approximate methods, such as the correlation expansion, are much more commonly used to study the combined dynamics of carriers and lattice vibrations in optically driven QDs.[1,2,30] Within the latter approach, one first sets up equations of motion for the occupation and the polarization. These equations are not closed, but are the starting point of an infinite hierarchy of higher-order phonon-assisted density matrices. This hierarchy has to be truncated by factorizing higher-order correlation functions on a chosen level. By including all density matrices with up to four operators, it has been shown that over a wide range of parameters, the correlation expansion is able to reproduce exactly known dynamics, both in the linear[1] and the nonlinear regime.[29] In the remainder of this paper, we aim to answer the open question of whether, and, if so, in which parameter range, the correlation expansion yields trustable results in the limit of long times. To this end, the numerically exact path-integral calculations can be used for benchmark purposes. A recent comparison between a fourth-order correlation expansion and the path-integral formalism concentrating on coherent control oscillations after excitation with two phase-locked pulses revealed that the correlation expansion breaks down at high temperatures and/or strong couplings.[36] However, in that work, the dynamics was studied only over a few ps. Having in mind that usually errors may accumulate during the evolution in time, one could expect that in the long-time limit, the parameter range, where the correlation expansion is applicable, shrinks compared with that found in Ref. 36. In contrast to this conclusion, here we will demonstrate that for a wide range of elevated temperatures and carrier-phonon coupling strengths, the correlation expansion yields surprisingly reliable predictions for the stationary nonequilibrium, even if it fails completely to reproduce the precedent dynamics. Problems in the long-time limit may, however, appear at low temperatures.

Let us first concentrate on the latter temperature regime and the weak-coupling limit, as represented by the unscaled GaAs carrier-phonon coupling strength. In this parameter range, two factors may limit the applicability of the correlation expansion: (i) The stationary state is reached after rather long times, i.e., fine-grained q discretizations are needed to ensure results that do not diverge over a long time interval. (ii) The memory introduced by the coupling to a continuum of acoustic phonons increases significantly with decreasing temperature, i.e., the dynamics is strongly non-Markovian. The latter dependence can be investigated using the path-integral approach and is illustrated in Fig. 6, where we show the stationary value of the off-diagonal element $\rho_{01}(\infty)$ as a function of temperature at field strengths of $f =$ (a) 0.5 and (b) 1.0 ps^{-1} for resonant excitation. As already stated above, in the implementation of the path-integral formalism, the memory truncation length can be varied. Plotted are results obtained by choosing different memory depths. For higher temperatures, the results for all displayed memory lengths coincide. However, in the range of low temperatures, significant deviations become apparent and the memory length that is chosen has to be rather long in order to ensure converged results, which are displayed as solid black

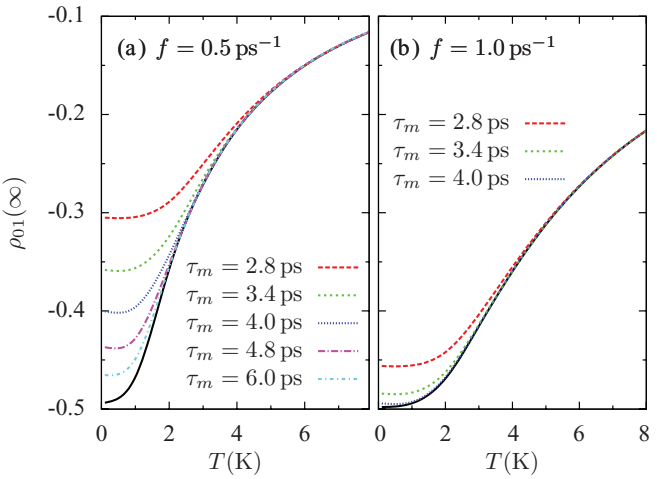

FIG. 6. (Color online) Stationary value of ρ_{01} as a function of temperature for field strengths of $f =$ (a) 0.5 and (b) 1.0 ps^{-1}. Colored lines correspond to different memory truncation lengths within the path-integral approach (see key); black lines represent converged results, i.e., they are unaffected if the memory is further increased.

lines. Here, by "converged"we mean that a further increase of the memory length does not lead to any further changes. Our results clearly demonstrate that the phonon-induced memory increases significantly for decreasing temperatures. In addition, a comparison between Figs. 6(a) and 6(b) reveals that the memory depth also noticeably depends on the strength of the optical driving and rises with decreasing laser intensities. Close to zero temperature, memory lengths of 9 and 5 ps, respectively, have to be chosen. The path-integral approach is capable of dealing with the long memory depths faced at low temperatures and weak fields. However, when fixing the time discretization, longer memory truncation lengths require a larger storage space, as well as longer computing times, and are thus much more demanding.

The corresponding results of the correlation expansion are added in Fig. 4 where they are displayed as squares. At $f = 1.0$ ps^{-1}, for nearly all temperatures, the correlation expansion agrees extremely well with the path-integral results (solid blue line), and confirms that Eq. (13a) overestimates the coupling-strength-related correction with respect to a thermal occupation of the dot-photon dressed states. Only in the range $T \lesssim 1$ K can slight deviations be found, which are probably due to the increased memory depths. At $f = 0.5$ ps^{-1} (red lines), the correlation expansion again coincides with the path integral at $T \geqslant 4$ K. However, due to the weak applied field strength for low temperatures, it takes very long times until the stationary state is reached.[3] In our calculations, even for the finest q discretization compatible with the computing power available to us for $T \leqslant 3$ K, the correlation expansion results diverged before this stationary limit was reached and, hence, no data points could be included in Fig. 4. Thus, for temperatures close to zero, the correlation expansion is not the method of choice to study the long-time behavior.

Let us finally turn to elevated temperatures and increased carrier-phonon couplings. Shown in Fig. 7 is the temporal evolution of the real part of ρ_{01} for $f = 1.0$ ps^{-1} at different

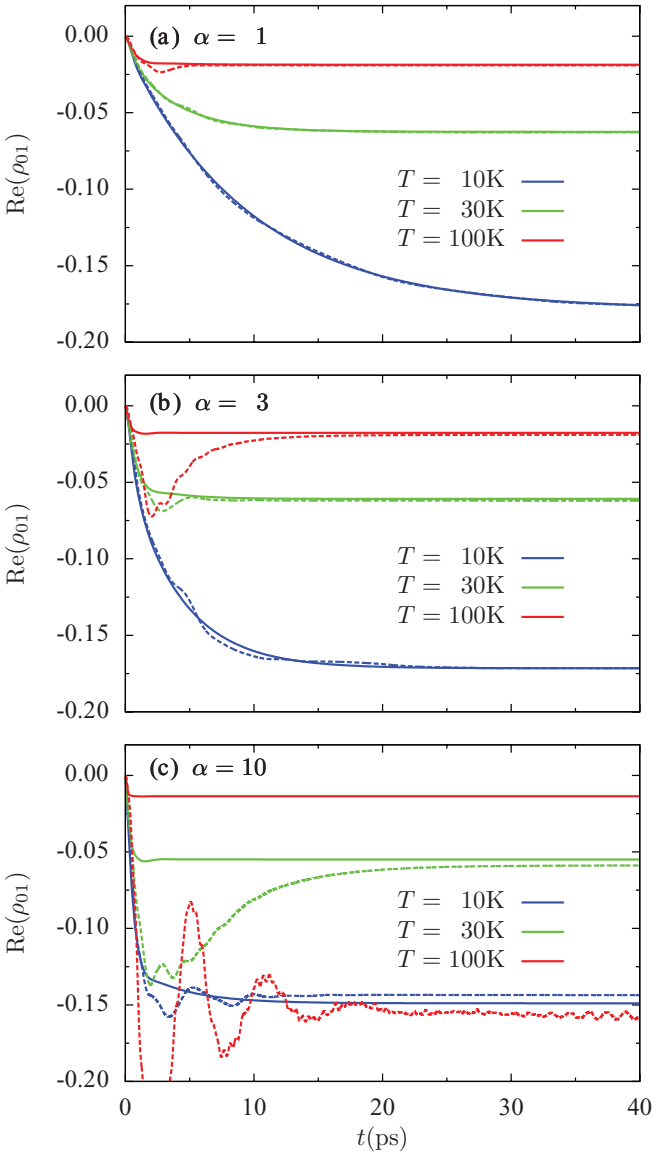

FIG. 7. (Color online) Time dependence of the real part of the coherence for $f = 1.0\ \mathrm{ps}^{-1}$ at different temperatures as indicated. Solid lines represent path-integral results; dashed lines correspond to a fourth-order correlation expansion. (a) Coupling constant of GaAs; (b) and (c) with $|\gamma_q|^2$ increased by factors of three and ten, respectively.

temperatures and coupling strengths. While in Fig. 7(a) the unscaled coupling constant of GaAs has been used, $|\gamma_{\mathbf{q}}|^2$ has been increased by factors of $\alpha = 3$ and 10 in Figs. 7(b) and 7(c), respectively. Solid lines display the path-integral calculations; dashed lines display the results of the correlation expansion. In the weak-coupling regime [Fig. 7(a)] for $T = 10$ and 30 K, the correlation expansion is in full agreement with the exact result. In particular, the long-time behavior is correctly reproduced. The latter holds also for $T = 100$ K, even when here, around $t = 3$ ps, the correlation expansion predicts a dip which is absent in the exact dynamics. For an intermediate coupling strength [Fig. 7(b)], deviations emerge during the evolution in time that are more pronounced for higher temperatures. For $T = 100$ K, the dynamics as predicted by the correlation expansion, after 1 ps, is already far off the exact result, and shows subsequently not only quantitative but marked qualitative deviations. However, these differences diminish in the course of time and the final long-time behavior is surprisingly close to the exact result. Before a stationary state is reached, even stronger discrepancies emerge in the strong-coupling regime [Fig. 7(c)], where the correlation expansion, at $T = 10$ K, already produces artificial oscillations. Nevertheless, despite these oscillations, the stationary state is still close to the path-integral result. A similar behavior can be found for $T = 30$ K. Only at $T = 100$ K does the correlation expansion disagree completely with the exact dynamics for all times longer than a few hundred fs. Thus, our comparison demonstrates that over a wide range of temperatures and coupling strengths, the correlation expansion yields rather reliable predictions in the long-time limit, even though for intermediate temperatures or coupling strengths the precedent dynamics cannot even qualitatively be reproduced.

IV. CONCLUSIONS

We analyzed the long-time dynamics of a continuously driven strongly confined quantum dot concentrating on pure dephasing processes due to the coupling to a continuum of acoustic phonons over a wide parameter range. Using numerically exact real-time path integrals enables us to characterize the stationary nonequilibrium of this many-particle system without any prejudice. We demonstrated that in the weak-coupling regime, even at high temperatures, the stationary state of the electronic system is close to a thermal occupation of the dot-photon dressed states, indicating that the role of phonons is restricted to provide a redistribution of the quasiparticle occupations. Indeed, our numerical results suggest that this description becomes exact in the limit of negligibly small carrier-phonon couplings. In the strong-coupling regime, the stationary values of the off-diagonal elements deviate significantly from a thermal occupation, reflecting that, here, phonons also contribute to the definition of the stable quasiparticles. It is found that the weak-coupling theory derived in Ref. 17 is capable of describing the tendencies of these deviations qualitatively, but overestimates the dependence on the coupling strength. Interestingly, the latter holds in particular in the weak-coupling regime, where the bare dressed-state assumption represents, for nearly all temperatures, a better estimate for the stationary nonequilibrium state. A comparison between path-integral results with different memory truncation lengths revealed that the memory of the system increases significantly with decreasing temperature and decreasing strength of the optical driving. For temperatures close to zero, the fairly long memory depths, which are specific to the superohmic coupling, may cause the rather large deviations of the weak-coupling theory from the exact result. If the laser frequency is shifted out of resonance, a stationary nonequilibrium close to a thermal occupation of the dot-photon dressed states leads to an interesting consequence: Depending on the sign of the detuning in the long-time limit, the QD occupation may exceed $\frac{1}{2}$, i.e., a higher final occupation is reached for off-resonant excitation than for resonant driving.

Using path-integral data for benchmark purposes, we studied the validity of a fourth-order correlation expansion.

We found that over a wide range of temperatures and carrier-phonon coupling strengths, the correlation expansion yields, in the long-time limit, surprisingly reliable results. Most interestingly, it predicts a stationary nonequilibrium state close to the exact result, even if it fails completely to reproduce the precedent dynamics, as seen for elevated temperatures or coupling strengths. As the correlation expansion is one of the most common approximative approaches to study the dynamics of correlated systems, our results may be useful in a wide range of physics.

ACKNOWLEDGMENTS

M. G. and M. D. C. acknowledge financial support by the Studienstiftung des Deutschen Volkes and the Alexander von Humboldt Foundation, respectively. P. M. acknowledges support from the Foundation for Polish Science under the TEAM programme, co-financed by the European Regional Development Fund. T. K. and P. M. acknowledge support from the Alexander von Humboldt Foundation within a Research Group Linkage Project.

*martin.glaessl@uni-bayreuth.de

[1] J. Förstner, C. Weber, J. Danckwerts, and A. Knorr, Phys. Rev. Lett. **91**, 127401 (2003).
[2] A. Krügel, V. M. Axt, T. Kuhn, P. Machnikowski, and A. Vagov, Appl. Phys. B **81**, 897 (2005).
[3] A. Vagov, M. D. Croitoru, V. M. Axt, T. Kuhn, and F. M. Peeters, Phys. Rev. Lett. **98**, 227403 (2007).
[4] A. J. Ramsay, A. M. Fox, M. S. Skolnick, A. V. Gopal, E. M. Gauger, B. W. Lovett, and A. Nazir, Phys. Rev. Lett. **104**, 017402 (2010).
[5] A. J. Ramsay, T. M. Godden, S. J. Boyle, E. M. Gauger, A. Nazir, B. W. Lovett, A. M. Fox, and M. S. Skolnick, Phys. Rev. Lett. **105**, 177402 (2010).
[6] D. P. S. McCutcheon and A. Nazir, New J. Phys. **12**, 113042 (2010).
[7] D. P. S. McCutcheon, N. S. Dattani, E. M. Gauger, B. W. Lovett, and A. Nazir, Phys. Rev. B **84**, 081305 (2011).
[8] P. Machnikowski and L. Jacak, Phys. Rev. B **69**, 193302 (2004).
[9] M. Glässl, M. D. Croitoru, A. Vagov, V. M. Axt, and T. Kuhn, Phys. Rev. B **84**, 125304 (2011).
[10] A. Nazir, Phys. Rev. B **78**, 153309 (2008).
[11] E. Biolatti, R. C. Iotti, P. Zanardi, and F. Rossi, Phys. Rev. Lett. **85**, 5647 (2000).
[12] P. Chen, C. Piermarocchi, and L. J. Sham, Phys. Rev. Lett. **87**, 067401 (2001).
[13] U. Bockelmann and G. Bastard, Phys. Rev. B **42**, 8947 (1990).
[14] P. Borri, W. Langbein, S. Schneider, U. Woggon, R. L. Sellin, D. Ouyang, and D. Bimberg, Phys. Rev. Lett. **87**, 157401 (2001).
[15] T. Takagahara, Phys. Rev. B **60**, 2638 (1999).
[16] A. Vagov, V. M. Axt, T. Kuhn, W. Langbein, P. Borri, and U. Woggon, Phys. Rev. B **70**, 201305(R) (2004).
[17] U. Weiss, *Quantum Dissipative Systems* (World Scientific, Singapore, 1999).
[18] A. J. Leggett, S. Chakravarty, A. T. Dorsey, M. P. A. Fisher, A. Garg, and W. Zwerger, Rev. Mod. Phys. **59**, 1 (1987).
[19] A. G. Redfield, IBM J. Res. Dev. **1**, 19 (1957).
[20] R. A. Harris and R. Silbey, J. Chem. Phys. **78**, 7330 (1983).
[21] H. Dekker, J. Phys. C: Solid State Phys. **20**, 3643 (1987).
[22] N. Makri and D. Makarov, J. Chem. Phys. **102**, 4600 (1995).
[23] N. Makri and D. Makarov, J. Chem. Phys. **102**, 4611 (1995).
[24] C. Meier and D. J. Tannor, J. Chem. Phys. **111**, 3365 (1999).
[25] Y. Dakhnovskii, Phys. Rev. B **49**, 4649 (1994).
[26] E. Sim, J. Chem. Phys. **115**, 4450 (2001).
[27] M. Thorwart, J. Eckel, and E. R. Mucciolo, Phys. Rev. B **72**, 235320 (2005).
[28] A. Vagov, M. D. Croitoru, M. Glässl, V. M. Axt, and T. Kuhn, Phys. Rev. B **83**, 094303 (2011).
[29] B. Krummheuer, V. M. Axt, and T. Kuhn, Phys. Rev. B **65**, 195313 (2002).
[30] F. Rossi and T. Kuhn, Rev. Mod. Phys. **74**, 895 (2002).
[31] L. DiCarlo, H. J. Lynch, A. C. Johnson, L. I. Childress, K. Crockett, C. M. Marcus, M. P. Hanson, and A. C. Gossard, Phys. Rev. Lett. **92**, 226801 (2004).
[32] J. R. Petta, A. C. Johnson, C. M. Marcus, M. P. Hanson, and A. C. Gossard, Phys. Rev. Lett. **93**, 186802 (2004).
[33] T. M. Stace, A. C. Doherty, and S. D. Barrett, Phys. Rev. Lett. **95**, 106801 (2005).
[34] C. Roy and S. Hughes, Phys. Rev. Lett. **106**, 247403 (2011).
[35] B. Krummheuer, V. M. Axt, T. Kuhn, I. D'Amico, and F. Rossi, Phys. Rev. B **71**, 235329 (2005).
[36] A. Vagov, M. D. Croitoru, V. M. Axt, P. Machnikowski, and T. Kuhn, Phys. Status Solidi B **248**, 839842 (2011).